Reactor sizing for butane steam reforming over Ni and Ru catalysts

Minjun Seong*, Mi Shin*, Jung-Ho Cho*, Young-Chul Lee**, Young-Kwon Park***, and Jong-Ki Jeon*,†

*Department of Chemical Engineering, Kongju National University, Cheonan 330-717, Korea
**R&D Division, Korea Gas Co., Ansan 426-860, Korea
***School of Environmental Engineering, University of Seoul, Seoul 130-743, Korea

Abstract−We obtained kinetics data on steam reforming of butane and calculated the appropriate reactor size based on the kinetics data. Using commercial Ni and Ru catalysts, steam reforming reactions of butane were performed while changing the reaction temperature and partial pressure of reactants. After comparing the power law model and the Langmuir-Hinshelwood model by using the kinetics data obtained from the experiment, it is revealed that the reaction rate could be determined by both models in the reforming reaction of butane over commercial Ni and Ru catalysts. Also, calculation of the steam reforming reactor size using a PRO/II simulation with a kinetic model equation showed that the reactor size using the Ni catalyst is smaller than that with the Ru catalyst to obtain the same conversion.
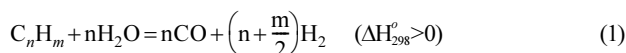
Keywords: Steam Reforming, Butane, Reaction Kinetics, Reactor Sizing, Simulation
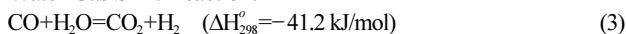
INTRODUCTION

Coal and oil have been the primary sources of energy for many different fields. However, alternative energy sources including natural gas, propane, and butane are also widely used in households and industry. One of the alternatives that is being considered is hydrogen, a clean source of energy that does not create pollution. Butane is one of the byproducts in petrochemical processes and refining, and is used as an energy source [1,2]. Using butane as a raw material for producing hydrogen instead of just burning it off would thus open new possibilities for using butane more effectively. Hydrogen can be obtained by performing a steam reforming reaction of hydrocarbon. The steam reforming reaction is widely used in hydrogen production facilities, fuel cell power generation systems, reforming reactors to obtain hydrogen from natural gas, and dimethyl ether processes [3-8].

The steam reforming process consists of a reforming reaction and water gas shift (WGS) reaction, according to Eqs. (1) to (3) [9].

Steam reforming reaction:

$$C_nH_m + nH_2O = nCO + \left(n + \frac{m}{2}\right)H_2 \quad (\Delta H^o_{298} > 0) \tag{1}$$

$$n-C_4H_{10} + 4H_2O = 4CO + 9H_2 \quad (\Delta H^o_{298} = 649.9 \text{ kJ/mol}) \tag{2}$$

Water Gas Shift Reaction:
$$CO + H_2O = CO_2 + H_2 \quad (\Delta H^o_{298} = -41.2 \text{ kJ/mol}) \tag{3}$$

The catalysts commonly used for the steam reforming reaction are Ni, Ru, and Rh [10]. Research on the kinetics for the steam reforming reaction has primarily focused on the methane steam reforming reaction [11-17]. The primary goal of obtaining kinetic data for

the reaction is to adequately express the chemical reaction as a kinetic model to design a reactor for commercial use. The kinetic model is thus a valuable tool for engineers to devise, optimize, and operate reactors. However, there have been few studies on kinetic models for the reformation of ethane, propane, or butane [19].

This study obtains kinetics data on steam reforming of butane and calculates the appropriate reactor size based on the kinetics data. Using commercial Ni and Ru catalysts, steam reforming reactions of butane were performed while changing diverse reaction conditions including reaction temperature, gas hourly space velocity (GHSV), a partial pressure of reactants. From the results, the most suitable kinetic model for steam reforming of butane was chosen. Reactor size, which depends on the reaction temperature under different catalysts including commercial Ni and Ru catalysts, was calculated by a simulation utilizing PRO/II.

EXPERIMENTAL

The catalysts used for the reaction include a commercial Ni catalyst (FCR-4; Süd-chemie Catalysts Inc., 12 wt% Ni/α-Al$_2$O$_3$) and a Ru catalyst (RuA; Süd-chemie Catalysts Inc., 2 wt% Ru/α-Al$_2$O$_3$), and each catalyst's BET surface area is 12.3 m^2/g$_{cat.}$ and 11.4 m^2/g$_{cat}$, respectively [20,21]. The catalyst used for the steam reforming reaction was ground into particles of around 75-100 μm size, and then used in the reaction. Before steam reforming was initiated, the catalyst was reduced in a stream of 10% hydrogen diluted in nitrogen gas. Ni catalysts were reduced for 2 hours at 500 °C, and Ru catalysts were reduced for an hour at 800 °C. In this study, hydrogen, nitrogen, and butane were utilized (the purity of each gas: 99.999% (Hydrogen), 99.999% (Nitrogen), and 99.5% (Butane).

Fig. 1 shows the experimental apparatus for the steam reforming reaction of butane. The reactor used in the reaction is a fixed bed reactor manufactured with quartz, and the reactor's inner diameter was 10 mm. to control the mass-flow rate of the gases (hydrogen, nitrogen, and butane), we used a mass flow controller. The mois-

†To whom correspondence should be addressed.
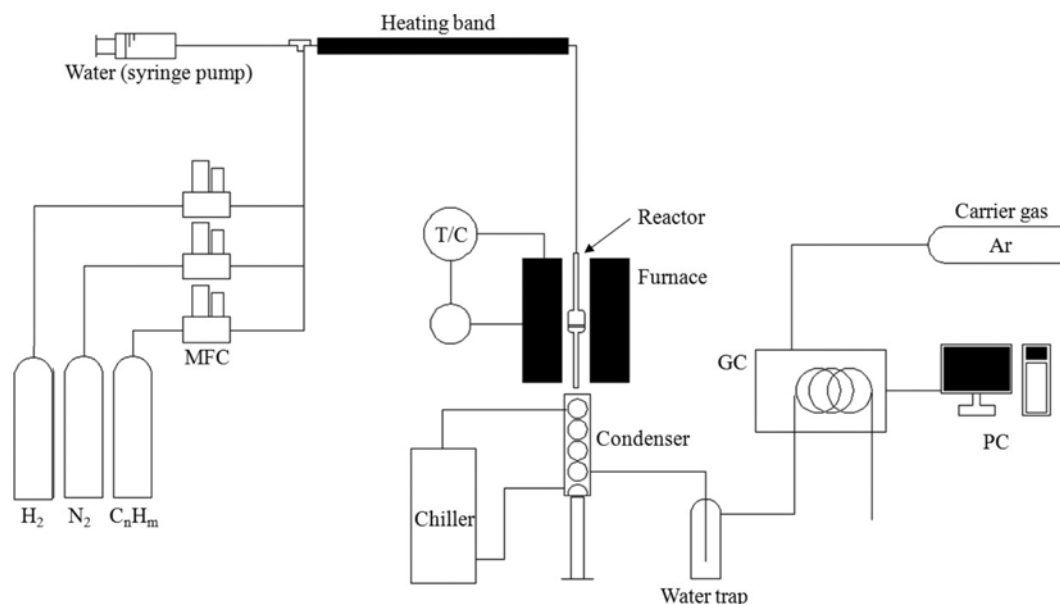E-mail: jkjeon@kongju.ac.kr

Fig. 1. Schematic diagram of experimental setup.

ture in the reaction products was eliminated by passing the product through a freezer and water trap, and analyzed by an on-line connected gas chromatography system with a methanizer (Model: Younglin, YL 6100 TOGA System). The columns used for the gas chromatography analysis were a Porapak N column and a molecular sieve 5A column. The detectors were a flame ionization detector and a thermal conductivity detector.

The steam reforming reaction experiment of butane was prepared by installing 0.1 g of the catalyst in the reactor. When a kinetic experiment is performed using a fixed-bed reactor, it is common to conduct the experiment with a differential reactor by changing the amount of catalysts or the reaction conditions, because integration is not necessary to obtain the reaction rate, thus making the derivation of the reaction rate much easier [22]. Therefore, we searched for reaction conditions where the conversion rate of butane gas would not exceed 10% at 350-450 °C, and performed the steam reforming reaction while maintaining the GHSV at 83,200 h^{-1} based on the flow rate of total gas.

RESULTS AND DISCUSSION

1. Kinetic Model for Steam Reforming of Butane

To obtain kinetic data for a chemical reaction, the experiment should be performed when the effect of surface diffusion is minimized, while the reactant passes through the catalyst layer [20]. Therefore, a preliminary experiment was conducted to determine an adequate catalyst size to obtain the best kinetic data. The sizes of the catalysts were divided into three categories (35-75 μm, 75-100 μm, and 100-125 μm) and were used for performing steam reforming reaction experiments according to the contact time. Since there was no significant difference in conversion rate upon change of the catalyst size, the reaction was not affected by internal diffusion limitation. Therefore, 75-100 μm was selected as the most appropriate catalyst size for the experiment.

The conversion of n-butane and selectivity obtained at different

Table 1. Conversion of n-butane and selectivity obtained at different feed over Ni and Ru catalysts at 400 °C

Catalyst	$P_{C_4H_{10}}$	P_{H_2O}	Conversion (%)	H_2/CO_2 molar ratio
Ni	0.12	0.50	8.77	3.18
	0.09	0.50	6.70	3.85
	0.06	0.50	4.60	4.92
	0.06	0.38	4.74	3.70
	0.06	0.67	4.26	3.92
Ru	0.12	0.50	7.87	3.17
	0.09	0.50	5.86	3.99
	0.06	0.50	4.06	4.20
	0.06	0.38	4.08	4.35
	0.06	0.67	4.02	4.40

feed over Ni and Ru catalysts at 400 °C are shown in Table 1. The product mixture is free of carbon monoxide, which indicates that carbon monoxide formation might have been suppressed by the water-gas shift reaction. The results are in agreement with the trends in a previous report on butane steam reforming over Ni-based catalysts [23] in that the product mixture has H_2/CO_2 molar ratio in a range of 3-5 and carbon monoxide is not detected. It is noticeable that the conversion of n-butane over the Ru catalyst was lower than that of Ni catalyst, which seems to be due to low content of Ru on Al_2O_3 compared with that of Ni on Al_2O_3.

Based on the data obtained from the kinetics experiments, we obtained a kinetic model equation that reflects the actual data. The kinetic model equation was derived using two methods, the power law model (P-L model), which can be simply expressed as a power law function, and the Langmuir-Hinshelwood model (L-H model), which considers the process of absorption and desorption between the reactant and active sites of the catalyst.

1-1. Derivation of the Power Law Model

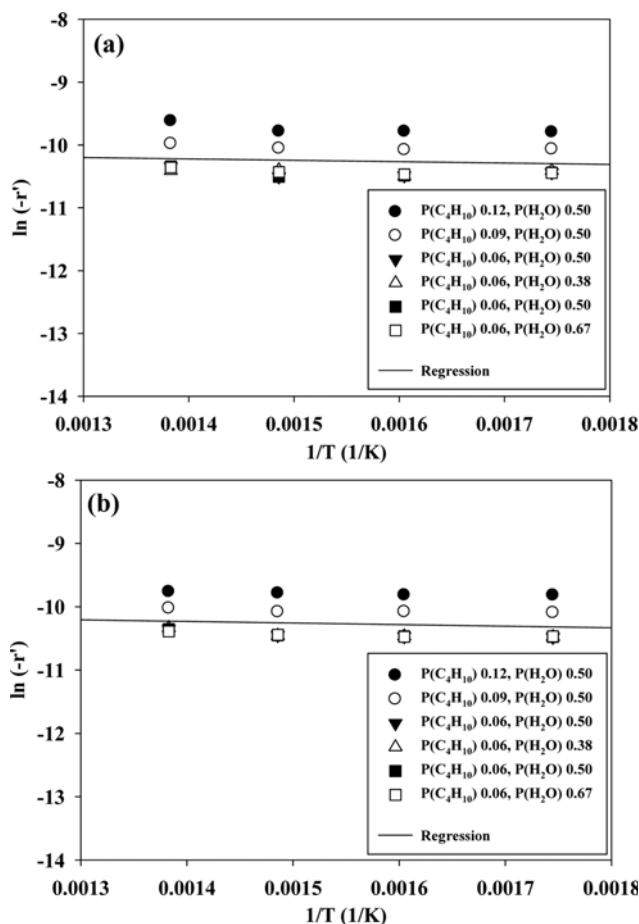To obtain the activation energy (E_a) included in the power law

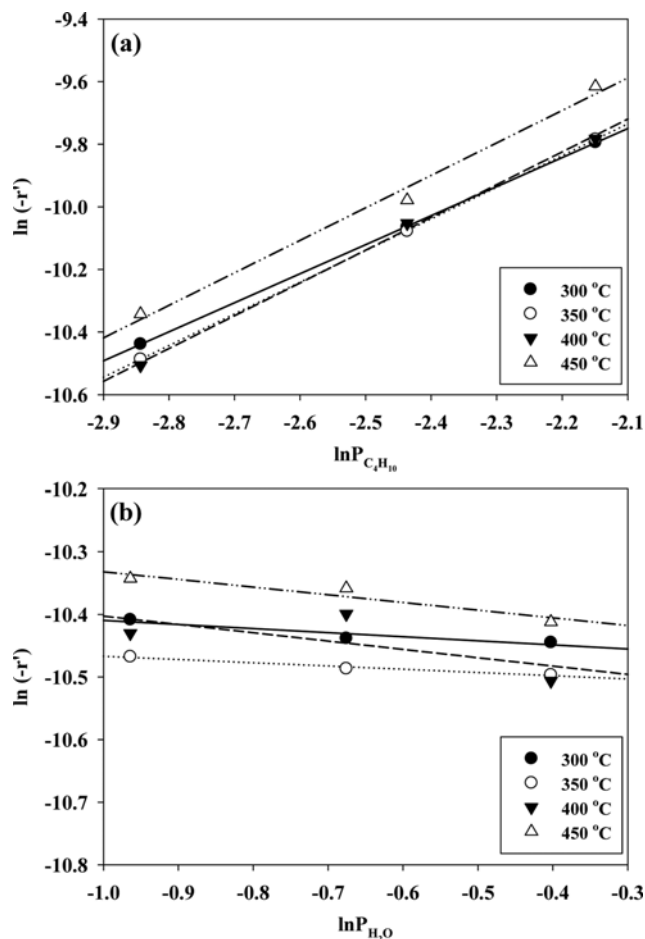**Fig. 2. Arrhenius plots of butane steam reforming over (a) Ni catalyst, (b) Ru catalyst.**

Fig. 3. Plots for reaction order of reactants in butane steam reforming over Ni catalyst: (a) reaction order of butane, (b) reaction order of steam.

model, the natural log of Eq. (4) is taken, which yields Eq. (5).

$$-r' = k_o \, EXP(-E_a/RT)[P_{C_4H_{10}}]^{\alpha}[P_{H_2O}]^{\beta} \qquad (4)$$

$$\ln(-r') = \ln(k_o[P_{C_4H_{10}}]^{\alpha}[P_{H_2O}]^{\beta}) - (E_a/R)(1/T) \qquad (5)$$

Under the conditions of reaction pressure of 1 atm, GHSV of 84,200 h^{-1}, and 2 hours of time-on-stream, the partial pressure of the steam (P_{H_2O}) was kept constant while the partial pressure of butane ($P_{C_4H_{10}}$) was varied from 0.06 to 0.12, and the change of the reaction rate with temperature change was plotted on a graph, as indicated in Fig. 2. Similarly, a graph expressing the relationship between the reaction rate and the temperature when keeping the partial pressure of butane ($P_{C_4H_{10}}$) constant while changing the partial pressure of the steam (P_{H_2O}) from 0.38 to 0.67 was also drawn in Fig. 2. In Fig. 2, a linear relationship is obtained when the x-axis was defined as (1/T) and the y-axis as ln($-r'$). From the slope of the graph, $-(E_a/R)$, the activation energy (E_a) was calculated. E_a for the Ni catalyst was 1.8 kJ/mol (Fig. 2(a)) and 2.1 kJ/mol when the Ru catalyst was used (Fig. 2(b)). The values indicated here are the average results obtained for the variation of partial pressure of the reactants.

Eq. (5) was rewritten to obtain the reaction orders of butane and steam from the reaction equation, and Eq. (6) was obtained:

$$\ln(-r') = \ln(k_o) - (E_a/R)(1/T) + \alpha\ln(P_{C_4H_{10}}) + \beta\ln(P_{H_2O}) \qquad (6)$$

To obtain the reaction order of butane (α), the partial pressure of the butane ($P_{C_4H_{10}}$) was varied while the partial pressure of steam (P_{H_2O}) was kept constant. Similarly, in order to obtain the reaction order of steam (β), the partial pressure of butane ($P_{C_4H_{10}}$) was kept constant when the partial pressure of steam (P_{H_2O}) was changed. The change in the reaction rate with change in partial pressure of either butane or steam is shown in Figs. 3 and 4, where the x and y axes represent the natural log value of partial pressure for each gas and the natural log value of the reaction rate, respectively. The average slope for each reaction temperature was used to obtain the reaction order. The reaction order for butane and steam was 1.01 and -0.09 for the Ni catalyst, respectively (Fig. 3), and 0.92 and -0.05 when the Ru catalyst was used, respectively (Fig. 4). Reaction orders show that the reaction rate is directly proportional to the partial pressure of n-butane, whereas a minor inhibition is expected at increased partial pressures of steam. The results are in agreement with the trends in previous report on butane steam reforming over Ni-based catalysts [23] in that a positive dependence on butane concentration and a negative dependence on steam concentration are observed.

The reaction rate constant (k) included in the power law model equation can be expressed as Eq. (7), by using the Arrhenius equation. By taking the natural log for both sides of Eq. (7), the pre-exponential factor can be derived from Eq. (8).
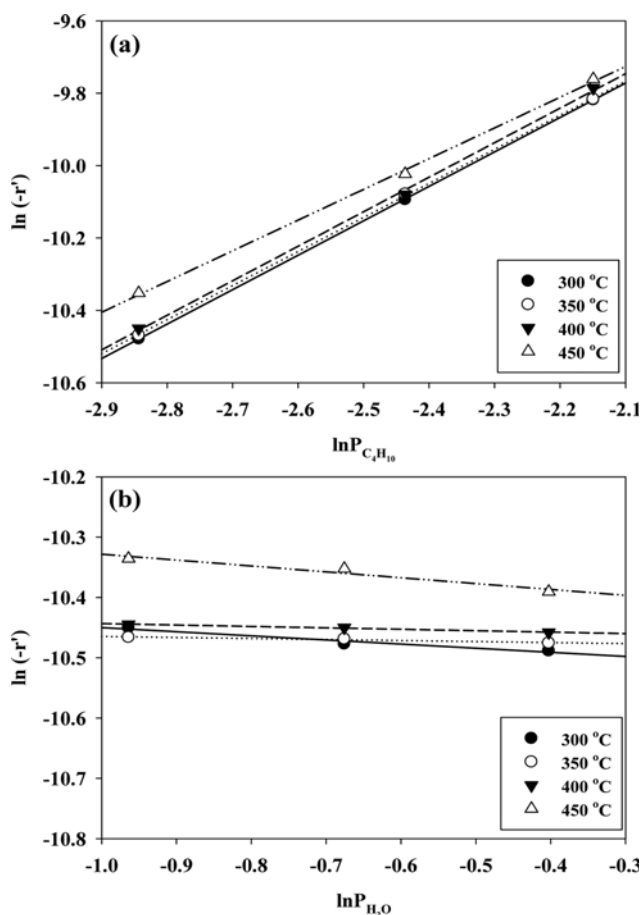
Fig. 4. Plots for reaction order of reactants in butane steam reforming over Ru catalyst: (a) reaction order of butane, (b) reaction order of steam.

Fig. 5. Plots for pre-exponential factor of butane steam reforming: (a) Ni catalyst, (b) Ru catalyst.

$$k = k_o \, EXP(-E_a/RT) \tag{7}$$

$$\ln(k) = \ln(k_o) - (E_a/R)(1/T) \tag{8}$$

Using a similar method as employed to obtain the activation energy (E_a), a linear relationship can be derived by setting the x-axis as (1/T) and the y-axis as ln (k). From the y-intercept of this graph, the pre-exponential factor (k_0) can be determined. The pre-exponential factor (k_0) derived from Fig. 5 was 0.79×10^{-3} for the Ni catalyst and 0.57×10^{-3} for the Ru catalyst. As a result, the activation energy (E_a) of butane, the reaction orders (α, β), and the pre-exponential factor (k_0) of the reaction order were obtained based on the power law model, and the results are summarized in Table 2.

1-2. Derivation of the Langmuir-Hinshelwood Model

The second kinetic model considered in this study is the Langmuir-Hinshelwood model (L-H model), which takes the adsorption mechanism between the active site of the catalyst and the reactant into account. The Langmuir-Hinshelwood model was used under the assumption that reactant molecules adsorb on active sites over the catalyst surface and the adsorbed molecules undergo a bimolecular reaction. The mechanism may be visualized as follows, where θ_i represents the fraction of available sites on which species i is adsorbed [22,24].
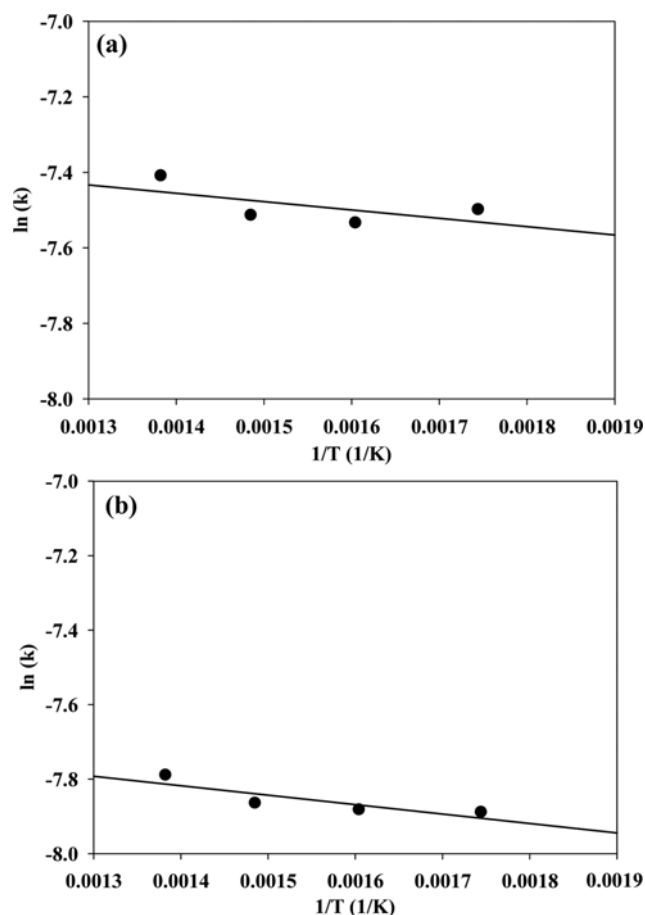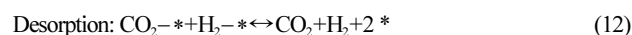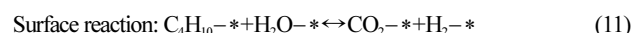
$$\text{Adsorption: } C_4H_{10} + * \leftrightarrow C_4H_{10} - * \tag{9}$$

Table 2. Parameter of butane steam reforming reaction for power law kinetic model

Catalyst	k_0	E_a [kJ/mol]	α	β
Ni	0.79×10^{-3}	1.8	1.01	-0.09
Ru	0.57×10^{-3}	2.1	0.92	-0.05

$$H_2O + * \leftrightarrow H_2O - * \tag{10}$$

$$\text{Surface reaction: } C_4H_{10} - * + H_2O - * \leftrightarrow CO_2 - * + H_2 - * \tag{11}$$

$$\text{Desorption: } CO_2 - * + H_2 - * \leftrightarrow CO_2 + H_2 + 2 * \tag{12}$$

At equilibrium, the rate of adsorption equals the rate of desorption, so that

$$k_{C_4H_{10}} P_{C_4H_{10}} \theta_v = k'_{C_4H_{10}} \theta_{C_4H_{10}}$$

$$\theta_{C_4H_{10}} = \left(\frac{k_{C_4H_{10}}}{k'_{C_4H_{10}}} \right) P_{C_4H_{10}} \theta_v = K_{C_4H_{10}} P_{C_4H_{10}} \theta_v \tag{13}$$

$$k_{H_2O} P_{H_2O} \theta_v = k'_{H_2O} \theta_{H_2O} \quad \theta_{H_2O} = \left(\frac{k_{H_2O}}{k'_{H_2O}} \right) P_{H_2O} \theta_v = K_{H_2O} P_{H_2O} \theta_v \tag{14}$$

$$k_{CO_2} P_{CO_2} \theta_v = k'_{CO_2} \theta_{CO_2} \quad \theta_{CO_2} = \left(\frac{k_{CO_2}}{k'_{CO_2}} \right) P_{CO_2} \theta_v = K_{CO_2} P_{CO_2} \theta_v \tag{15}$$

$$k_{H_2} P_{H_2} \theta_v = k'_{H_2} \theta_{H_2} \quad \theta_{H_2} = \left(\frac{k_{H_2}}{k'_{H_2}} \right) P_{H_2} \theta_v = K_{H_2} P_{H_2} \theta_v \tag{16}$$

If the surface reaction is the rate determining step, the reaction rate for the Langmuir-Hinshelwood model in steam reforming of butane can be expressed as Eq. (17):

$$r = k_S \theta_{C_4H_{10}} \theta_{H_2O} \tag{17}$$

Adding Eqs. (13)-(16),

$$\theta_v(K_{C_4H_{10}}P_{C_4H_{10}} + K_{H_2O}P_{H_2O} + K_{CO_2}P_{CO_2} + K_{H_2}P_{H_2})$$
$$= \theta_v + \theta_v + \theta_v + \theta_v = 1 - \theta_v \tag{18}$$

$$\theta_v = 1/(1 + K_{C_4H_{10}}P_{C_4H_{10}} + K_{H_2O}P_{H_2O} + K_{CO_2}P_{CO_2} + K_{H_2}P_{H_2}) \tag{19}$$

Combining Eqs. (13), (14), (17), and (19) gives

Table 3. Parameters for the Langmuir-Hinshelwood model

Catalyst	Temperature [°C]	k_s	$K_{C_4H_{10}}$	K_{H_2O}
Ni	350	0.000549	0.413	1.011
	400	0.000564	1.048	0.772
	450	0.000577	1.696	3.355
Ru	350	0.000379	7.400	9.289
	400	0.000391	7.139	8.870
	450	0.000401	7.752	9.476

$$r = k_S K_{C_4H_{10}} K_{H_2O} P_{C_4H_{10}} P_{H_2O}$$
$$/(1 + K_{C_4H_{10}}P_{C_4H_{10}} + K_{H_2O}P_{H_2O} + K_{CO_2}P_{CO_2} + K_{H_2}P_{H_2})^2 \tag{20}$$

In this equation, k_s is a constant expressing the characteristics of the surface reaction, and the constants $K_{C_4H_{10}}$ and K_{H_2O} are adsorption equilibrium constants for butane and steam, respectively. If the adsorption of reaction products is very weak, the last two terms in the denominator can be deleted, and Eq. (20) would become [19]

$$-r'_{C_4H_{10}} = k_S K_{C_4H_{10}} K_{H_2O} P_{C_4H_{10}} P_{H_2O}/(1 + K_{C_4H_{10}}P_{C_4H_{10}} + K_{H_2O}P_{C_4H_{10}})^2 \tag{21}$$

After measuring the reaction rate according to the change in partial pressure of butane and steam in a temperature range of 350-450 °C, the Polymath program was used to perform a non-linear regression to compute the unknown constants k_s, $K_{C_4H_{10}}$, and K_{H_2O}, in Eq. (21). The parameters for the steam reforming reaction of butane at a temperature range of 350-450 °C for the Langmuir-Hinshelwood model are in Table 3.

1-3. Comparison of the Power Law Model and the Langmuir-Hinshelwood Model

The data from the experiments and the two models, the power law model and the Langmuir-Hinshelwood model, were compared with each other. The equations for both models and experimental
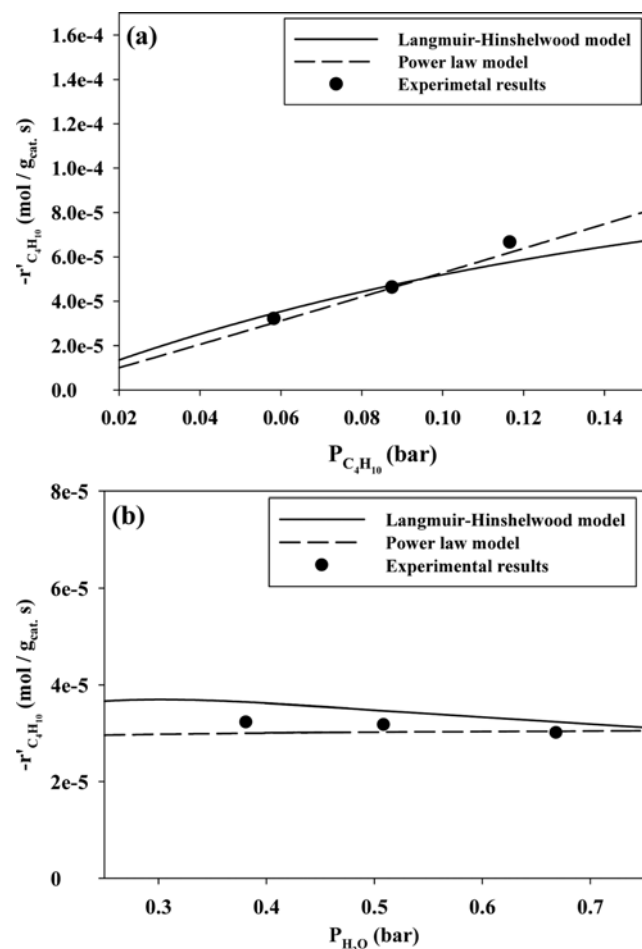

Fig. 6. Comparison of the kinetic model evaluation in butane steam reforming over Ni catalyst: (a) constant concentration of steam, (b) constant concentration of butane).
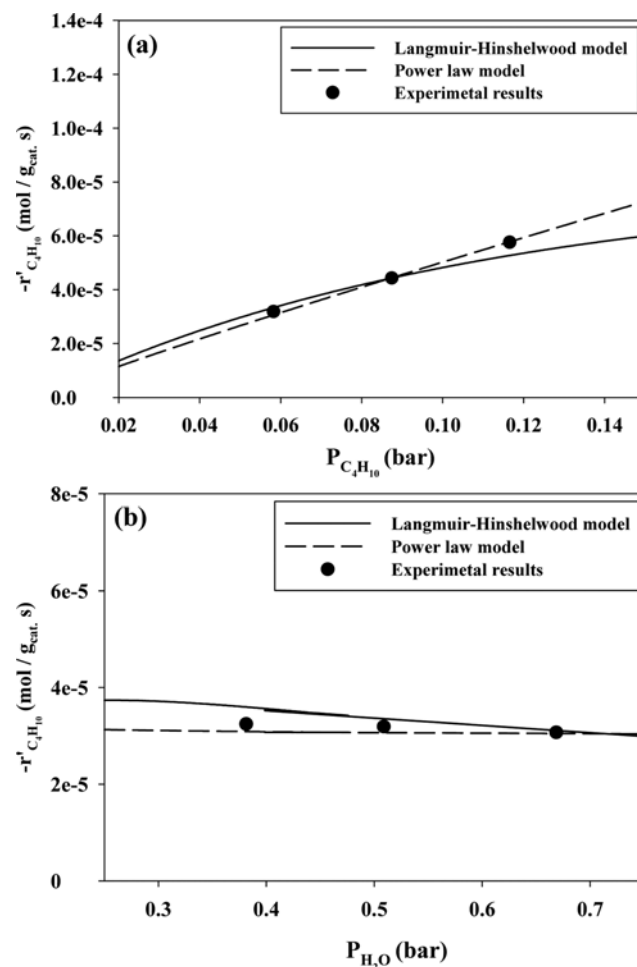

Fig. 7. Comparison of the kinetic model evaluation in butane steam reforming over Ru catalyst: (a) constant concentration of steam, (b) constant concentration of butane).

data obtained at 450 °C over Ni and Ru catalysts are shown in Fig. 6 and 7, respectively. The experiment with variation of the partial pressure of butane under Ni and Ru catalysts (Fig. 6(a), Fig. 7(a)) and the experiment changing the partial pressure of the steam (Fig.6(b), Fig. 7(b)) showed similar results to the Langmuir-Hinshelwood model as well as the power law model. As a result of the reforming reaction of butane over commercial Ni and Ru catalysts, the reaction rate could be determined by the power law model as well as the Langmuir-Hinshelwood model.

1-4. Kinetic Equation for Water Gas Shift Reaction

The water gas shift reaction is described in Eq. (3), where carbon monoxide that is produced after the steam reforming reaction reacts with steam and converts into carbon dioxide and hydrogen. To derive the power law model parameters for the WGS reaction, the experiments were performed in a similar manner as the steam reforming reaction of natural gas. From the experimental results, the activation energy (E_a), reaction order (α, β), and per-exponential factor (k_o) were derived. Eqs. (22) and (23) are the reaction rate equations over the Ni and Ru catalysts, respectively.

$$-r_{CO} = 8.42 \times 10^{-6} * EXP(-14.8 \times 10^{3}/(8.314 * T))$$
$$* [C_{CO}]^{0.0} * [C_{H_2O}]^{-0.2} \quad (22)$$

$$-r_{CO} = 1.21 \times 10^{-3} * EXP(-24.4 \times 10^{3}/(8.314 * T))$$
$$* [C_{CO}]^{0.6} * [C_{H_2O}]^{-0.1} \quad (23)$$

2. Reactor Sizing for Steam Reforming of Butane over Ni and Ru Catalysts

The reactor size was determined by using a PRO/II simulation program using the model equation obtained based on the kinetics data. The parameters that were entered to compute the reactor size for the steam reforming reaction are indicated in Table 4. The Lang-

Table 4. Input data for steam reforming reactor sizing by PRO/II simulation program

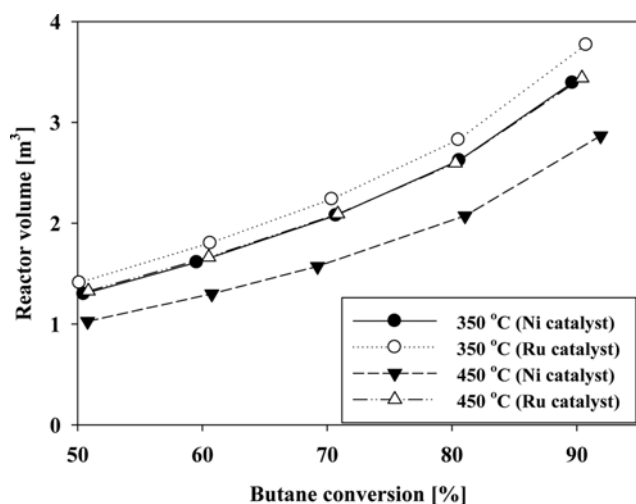| Catalyst	Feed component flow rate (gas phase) [m^3/h]			
	F_{N_2}	$F_{C_4H_{10}}$	F_{H_2O}	F_{total}
Ni or Ru	293.14	1.86	16.24	311.24

Fig. 8. Effect of butane conversion on reactor volume in butane steam reforming.

muir-Hinshelwood model equation was used for the simulation along with its parameters. A fixed bed catalyst reactor was assumed, with a stream of mixed gas that contains 0.94% of butane, similar to the amount of butane in natural gas, injected with a mass-flow rate of 311 m^3/h, and the steam was also injected to provide a steam/carbon ratio of 2.0 to simulate the reaction. In this simulation, the reactor's volume was determined from the weight, the density, and the porosity of the catalysts, and the conversion rate of butane was calculated using the PRO/II simulation program after the obtained kinetic model equation was applied. The reactor's size to accomplish the conversion rate of butane under commercial Ni and Ru catalysts using the Langmuir-Hinshelwood model is indicated in Fig. 8. As the reaction temperature increases, the reactor volume for the process becomes smaller, and the reactor has to be of a very large volume in order to have a higher conversion rate of butane. The reactor volume required to reach a certain level of hydrogen production at reaction temperature of 350-450 °C was smaller in the reactor using the Ni catalyst than the reactor using the Ru catalyst. Therefore, if only the reactor size is compared, using the Ni catalyst is more economical than using the Ru catalyst in steam reforming of butane at a temperature range of 350-450 °C.

CONCLUSIONS

The kinetics data of steam reforming of butane were obtained over commercial Ni and Ru catalysts while changing reaction temperature and the partial pressure of butane and steam. After comparing the power law model and the Langmuir-Hinshelwood model by using the kinetics data obtained from the experiment, it is revealed that the reaction rate could be determined by both models in the reforming reaction of butane over commercial Ni and Ru catalysts. Also, calculation of the steam reforming reactor size using a PRO/II simulation with the proposed kinetic model equation showed that the reactor size using the Ni catalyst is smaller than that with the Ru catalyst to obtain the same conversion rate.

ACKNOWLEDGEMENT

REFERENCES

1. T. Ren, B. Daniels, M. K. Patel and K. Blok, *Resour. Conserv. Recycl.*, **53**, 653 (2009).
2. T. Ren and M. K. Patel, *Resour. Conserv. Recycl.*, **53**, 513 (2009).
3. C. H. Park, K. S. Kim, J. W. Jun, S. Y. Cho and Y. K. Lee, *J. Korean Ind. Eng. Chem.*, **20**, 186 (2009).
4. A. J. Vizcaino, A. Carrero and J. A. Calles, *Int. J. Hydrog. Energy*, **32**, 1450 (2007).
5. T. S. Christensen, *Appl. Catal. A: Gen.*, **138**, 285 (1996).
6. P. O. Graf, B. L. Mojet, J. G. van Ommen and L. Lefferts, *Appl. Catal. A: Gen.*, **332**, 310 (2007).
7. Z. Y. Huang, C. H. Xu, C. Q. Liu, H. W. Xiao, J. Chen, Y. X. Zhang and Y. C. Lei, *Korean J. Chem. Eng.*, **30**, 587 (2013).
8. P. Kuchonthara, B. Puttasawat, P. Piumsomboon, L. Mekasut and T. Vitidsant, *Korean J. Chem. Eng.*, **29**, 1525 (2012).

9. T. Sperle, D. Chen, R. Lødeng and A. Holmen, *Appl. Catal. A: Gen.*, **282**, 195 (2005).

10. B. T. Schädel, M. Duisberg and O. Deutschmann, *Catal. Today*, **142**, 42 (2009).

11. J. H. Jeong, J. W. Lee, D. J. Seo, Y. Seo, W. L. Yoon, D. K. Lee and D. H. Kim, *Appl. Catal. A: Gen.*, **302**, 151(2006).

12. L. P. R. Profeti, E. A. Ticianelli and E. M. Assaf, *Fuel*, **87**, 2076 (2008).

13. K. Hou and R. Hughes, *Chem. Eng. J.*, **82**, 311 (2001).

14. S. S. Maluf and E. M. Assaf, *Fuel*, **88**, 1547 (2009).

15. M. Leventa, D. J. Gunn and M. A. El-Bousi, *Int. J. Hydrog. Energy*, **28**, 945 (2003).

16. V. R. Choudhary and K. C. Mondal, *Appl. Energy*, **83**, 1024 (2006).

17. Z. A. Aboosadi, M. R. Rahimpour and A. Jahanmiri, *Int. J. Hydrog. Energy*, **36**, 2960 (2011).

18. M. Zeppieri, P. L. Villa, N. Verdone, M. Scarsella and P. D. Filippis, *Appl. Catal. A: Gen.*, **387**, 147 (2010).

19. W. H. Lee, Master Dissertation, Kongju National University, Gongju, Korea (2011).

20. Y. Zhan, D. Li, K. Nishida, T. Shishido, Y. Oumi, T. Sano and K. Takehira, *Appl. Catal. A: Gen.*, **356**, 231 (2009).

21. D. Li, K. Nishida, Y. Zhan, T. Shishido, Y. Oumi, T. Sano and K. Takehira, *Appl. Clay Sci.*, **43**, 49 (2009).

22. H. Chon and G. Seo, *Introduction of catalysis*, Hanrimwon, Seoul (2002).

23. A. K. Avcı, D. L. Trimm, A. E. Aksoylu and Z. I. Önsan, *Appl. Catal. A: Gen.*, **258**, 235 (2004).

24. C. N. Satterfield, *Heterogeneous catalysis in industrial practice*, McGraw-Hill, Inc., New York (1993).